A plastic phase of water from computer simulation

Yoshio Takii, Kenichiro Koga, and Hideki Tanaka[a]

Department of Chemistry, Okayama University, 3-1-1 Tsushima-naka, Okayama 700-8530, Japan

We report a member of ices called plastic or rotator phase, in which individual water molecules make facile rotations as in liquid state but are held tightly in an ordered structure. Molecular dynamics simulations of three classical models of water show that a plastic ice phase appears at a temperature when ice VII is heated or liquid water is cooled at high pressures above several gigapascals. A large amount of latent heat is absorbed when ice VII is transformed to the rotator phase at 590 K and 10 GPa, which is a typical characteristic of the plastic transitions for nearly spherical molecules. In addition to the spontaneous formation of plastic phase in the simulations, its existence is supported by robustness of plastic phase for hypothetical water with varying degrees of Coulombic interactions. © *2008 American Institute of Physics.* [DOI: 10.1063/1.2927255]

I. INTRODUCTION

Water has a rich variety of polymorphs in a wide range of temperature and pressure. Structure and stability of most ice phases are accounted for in terms of four strong hydrogen bonds for each molecule.[1,2] Recent studies of water have uncovered intriguing properties of water in extreme conditions and biologically relevant systems such as deeply supercooled states,[3] very high pressures,[4,5] and nanoscale confinements.[6,7] For pressures lower than 20 GPa, the molecular framework of water is well preserved so that its morphology and properties are dominated by its most striking feature to form hydrogen bonds with four neighbors.[4,5] One of the examples is a theoretical study of water in a carbon nanotube,[6] which found that water molecules form ordered stacked-ring structures, called ice nanotube, in which each molecule forms four hydrogen bonds with its neighbors as in bulk ices in spite of the large deviation in the hydrogen-bond angle from the ideal one. The predicted ices in carbon nanotubes were later confirmed by experiments,[8,9] which in turn demonstrate high reliability of molecular dynamics (MD) simulation and the intermolecular interaction for water.

High-pressure ice VII and its proton-ordered form ice VIII occupy a large domain in a temperature-pressure phase diagram of water. Ice VII has a body-centered cubic (bcc) structure composed of two interpenetrating low pressure cubic ice lattices, and so it has the highest density among ices made of intact H_2O molecules. A comprehensive computer simulation study of ice phases showed that the TIP4P potential[10] is capable of reproducing the most part of the phase diagram correctly.[11] The only qualitative difference from the experiment is the slope of the phase boundary between ice VII and VIII in the temperature-pressure plane; it is vertical or negative in experiment,[2] while it is positive in simulation.[11] The origin of this discrepancy is, we hope, addressed in the present study.

A plastic phase is an unusual solid state found for some substances in which molecules rotate nearly freely at lattice sites.[12] A plastic phase of water, if any, would have a fairly high density. This is because diffusional motions can be hindered by the packing such that the temperature at which molecules start to make free rotations becomes lower than the temperature at which they start to diffuse by translational motions, i.e., the melting temperature. Such a dense packing is realized in ice VII and we report below the existence of a plastic phase for several models of water. Appearance of a plastic phase arises from nearly spherical shape of a water molecule.

In the following study, we perform constant temperature (T) and pressure (p) MD simulations of water[13,14] to examine thermodynamic properties, structure, and dynamics of water. Phase behavior of ice VII is investigated in several series of the MD simulations, each series corresponding to an isobaric path in the T-p phase diagram.

II. SIMULATION METHOD

Initial structure of ice VII is so prepared as to satisfy the Bernal–Fowler rule with zero net polarization.[1,2] The intermolecular interactions are described by one of three kinds of the potentials, known as TIP5P, TIP4P, and SPC/E.[10,15,16] We are mainly concerned with the results of the TIP5P potential. Use of the rigid molecules is justified by experimental observations that an individual molecule in ice remains intact up to 20 GPa with negligible pressure dependence of its OH chemical bond length.[4,5]

In the first series of MD simulations, the initial structure is taken to be a generated ice VII structure. After a very short run (40 ps) with a fixed density, a long equilibration run is performed at constant temperature and pressure. In the second series, the initial structure is either crystal, plastic, or liquid obtained from the first series, and equilibration runs start at various temperatures and pressures. A cubic box subject to the periodic boundary condition contains 432 water molecules in each simulation. We also examine larger systems containing 1024 and 3456 molecules. Totally we have performed more than 500 MD simulations in various condi-

tions and potential models, each lasting at least for 4 ns with a time step of 0.4 fs and in some cases for 25 ns. Convergence to a stable phase is completed within 1 ns in most cases and it takes a few nanoseconds in cases in which the thermodynamic state is close to a stability limit. After elapsing of 4 ns, no transformation is observed. The potential is either truncated smoothly at 0.86 nm or corrected by the Ewald sum method, which takes account of the long range Coulombic interaction.[17,18]

To calculate the free energy of liquid water and plastic ice, the thermodynamic integration method is applied. This method has been successfully used for free energy calculations of various liquids. With this method, the free energy can be calculated for any system with the potential energy function of the form

$$\Phi(\lambda) = \Phi_0 + \lambda^k(\Phi_1 - \Phi_0), \tag{1}$$

where Φ_0 is the potential energy function of a reference system whose free energy is known and Φ_1 is the potential energy function of the system of interest. In Eq. (1), k is generally a positive integer ($k \geq 2$) and λ is a coupling parameter; $\lambda = 0$ corresponds to the reference system and $\lambda = 1$ corresponds to the system of interest. In the simulation, $\langle \partial U(\lambda)/\partial \lambda \rangle_{N,V,T,\lambda}$ is calculated for various λ values from $\lambda = 0$ to $\lambda = 1$, which gives the Helmholtz free energy difference between the reference and the system of interest as

$$\Delta A = \int_0^1 \left\langle \frac{\partial \Phi(\lambda)}{\partial \lambda} \right\rangle_{N,V,T,\lambda} d\lambda, \tag{2}$$

where $\langle \ \rangle_{N,V,T,\lambda}$ denotes the ensemble average taken under fixed number of molecules N, volume V, temperature T, and the coupling parameter λ.[19] The volume is set to the mean volume that has been obtained in NpT ensemble MD simulation at a given pressure p.

For liquid water, the ideal gas of rigid nonlinear molecules is the reference system. Thus, in Eq. (1), $\Phi_0 = 0$. In addition, $k = 8$ is chosen here for calculating the free energy of liquid water. Note that, for the ideal gas, the Helmholtz free energy can be written in an analytical form

$$A_0 = Nk_BT\left(\ln \rho - 1 + \ln \Lambda^3 - \ln\left[\frac{\pi^{1/2}}{\sigma}\left(\frac{8\pi^2 I_A k_B T}{h^2}\right)^{1/2}\right.\right.$$
$$\left.\left. \times \left(\frac{8\pi^2 I_B k_B T}{h^2}\right)^{1/2}\left(\frac{8\pi^2 I_C k_B T}{h^2}\right)^{1/2}\right]\right), \tag{3}$$

where k_B is the Boltzmann constant, ρ is the density of liquid water, Λ is the thermal wave length, I_A, I_B, and I_C are the principal moments of inertia of a water molecule, and the symmetry number σ is 2. Once the Helmholtz free energy is known, the Gibbs free energy can be calculated via $G = A + p\langle V \rangle$, where $\langle V \rangle$ is the equilibrium volume obtained from the NpT simulation.

For plastic solid, the reference system is chosen to be a collection of Einstein oscillators whose individual frequency is set to ν_0 (corresponding to 75 cm^{-1}) in translational motion and to be a free rigid rotor in rotational motion as

$$A_0 = U_q(V) + 3Nk_BT\ln(h\nu_0/k_BT)$$
$$- Nk_BT \ln\left[\frac{\pi^{1/2}}{\sigma}\left(\frac{8\pi^2 I_A k_B T}{h^2}\right)^{1/2}\right.$$
$$\left. \times \left(\frac{8\pi^2 I_B k_B T}{h^2}\right)^{1/2}\left(\frac{8\pi^2 I_C k_B T}{h^2}\right)^{1/2}\right], \tag{4}$$

where $U_q(V)$ is the potential energy of the system in equilibrium position at a temperature of 0 K. The same method as in liquid is applied with $k = 6$.

The Helmholtz free energy of ice VII, which is a function of T and V, can be expressed as

$$A(T,V) = U_q(V) + F_h(T,V) + F_a(T,V) - TS_c, \tag{5}$$

where $F_h(T,V)$ and $F_a(T,V)$ are the harmonic vibrational free energy and anharmonic vibrational free energy, respectively. S_c stands for the residual entropy and is given by $k_BN \ln\left(\frac{3}{2}\right)$ for a proton-disordered system of N molecules. The harmonic vibrational free energy is given by
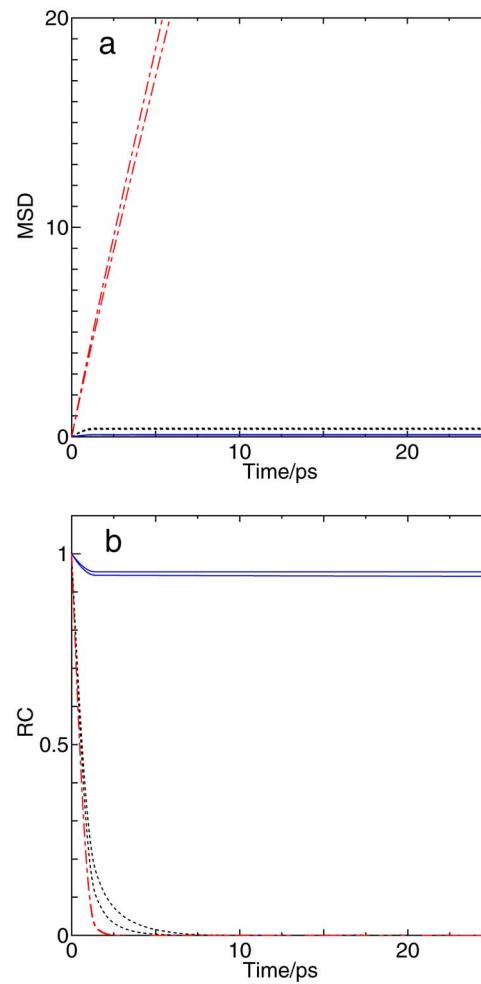
FIG. 1. (Color online) Time-dependent properties at 8 GPa and densities of water. (a) MSD in $(0.1 \text{ nm})^2$ on translations, (b) RC on rotations at 400 and 440 (blue, solid), 560 and 600 K (black, dotted), 760 and 780 K (red, dash dot).

$$F_h(T,V) = k_B T \sum_i \ln(h\nu_i/k_B T), \qquad (6)$$

where ν_i is the ith mode frequency. These frequencies are obtained by diagonalizing the mass weighted force constant matrix. The anharmonic vibrational free energy can be determined from the relation

$$\frac{F_a(T,V)}{T} = -\int_0^T \frac{U_a}{T'^2} dT', \qquad (7)$$

where U_a is the anharmonic vibrational energy. U_a is given by

$$U_a = U - U_q - U_h, \qquad (8)$$

where U is the potential energy calculated from MD simulation in the NTV ensemble and U_h is the harmonic vibrational energy, which is given by $6Nk_B T$.

III. RESULTS and DISCUSSION

The first series of simulations are carried out with the TIP5P model of water, which has four charged and one Lennard-Jones (LJ) sites.[15] Thermodynamic states along isobaric paths of 5–12 GPa are examined by increasing T in steps of 20 K in the range from 400 to 900 K, where an initial simulation starts with the ice VII structure prepared. Both static and dynamic properties at 8 GPa change abruptly at two temperatures, 550 and 760 K. Figures 1(a) and 1(b) show two dynamic properties associated with translational and rotational motions at these temperatures, i.e., mean square displacements (MSDs) $\langle [\mathbf{R}(t) - \mathbf{R}(0)]^2 \rangle$ and the reorientational correlations (RCs) $\langle \mathbf{u}(t) \cdot \mathbf{u}(0) \rangle$, where $\mathbf{R}(t)$ and $\mathbf{u}(t)$ stand for a center of mass coordinate and a unit vector parallel to a dipole of each water molecule at time t, and the

average $\langle \cdots \rangle$ is taken over all molecules and the time origin. The slope of the MSD, which is a measure of diffusivity, is nearly zero up to 750 K, suggesting that the translational motions are limited to vibrations around the lattice sites. (Occasional jumplike motions above 600 K give rise to a small but finite slope, which is observed for certain plastic phases.[12,20]) The RC stays around 0.95 at low temperatures due to librational motions of water molecules, whereas it decays rapidly to zero at $T=560$ K. The latter, together with the nearly zero slope of MSD, indicates that each water molecule rotates without diffusing from its lattice site; this is by definition a plastic phase. With increasing T, the plastic phase appears at 560 K and becomes unstable and melts at 760 K where the system has a nonzero slope in MSD with the fast decay in RC, i.e., it turns into a liquid state, acquiring diffusional motions. The rotational relaxation time in the plastic phase is an order of picoseconds, which is only slightly shorter than that in the liquid state at 760 K.

Molecular arrangements in ice VII, plastic, and liquid are depicted in Fig. 2, which are those free from thermal noise, called local energy minimum or inherent structures.[21] In plastic phase, the translational symmetry is essentially the same as that in crystalline ice VII, i.e., the arrangement of oxygen atoms does not change upon transition, but that of protons does change significantly. The plastic phase is easily discriminated from the other two phases by not only dynamic but also thermodynamic properties. The peak positions in radial distribution function depicted in Fig. 2(d) also suggest that positions of oxygen atoms in plastic phase are essentially the same as those in crystalline structure, although lower peaks in plastic phase are caused by winding of oxygen alignment. The peak positions in liquid state around 700 K obtained by *ab initio* MD study agree well with the
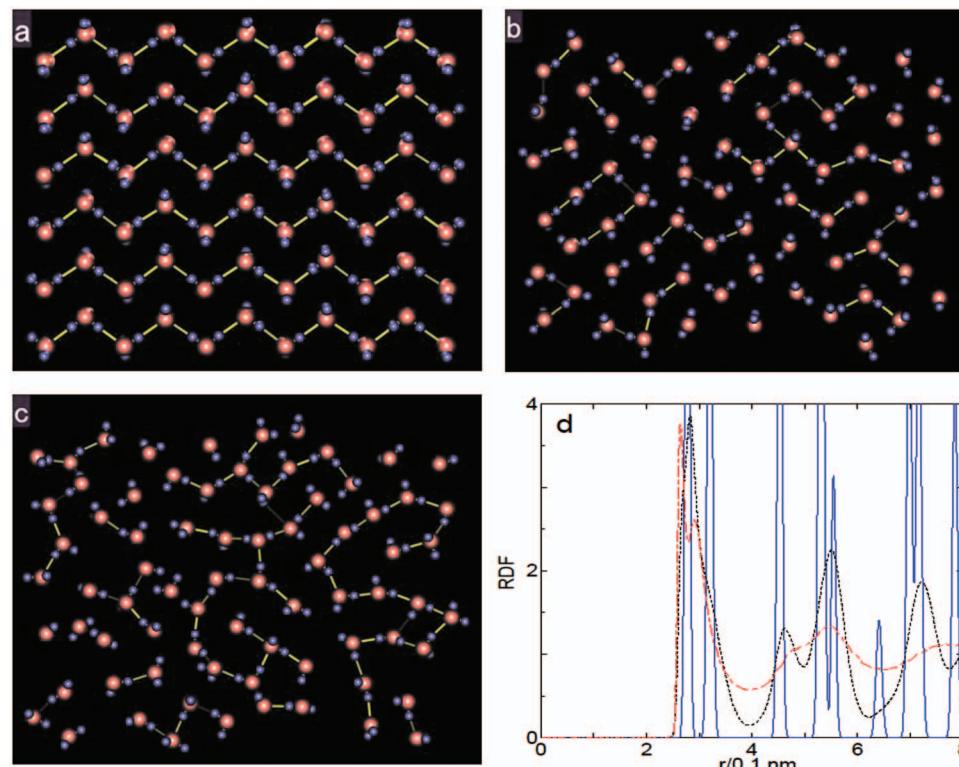
FIG. 2. (Color) (a) Molecular arrangements in the (1,1,0) plane (two layers only) removing thermal motions, corresponding to crystal at 420 K, (b) plastic at 600 K, and (c) liquid at 780 K. Hydrogen bonds are shown by yellow lines. (d) O–O radial distribution functions in inherent structure at 420 K (blue, solid), 600 K (black, dotted), and 780 K (red, dash dot).
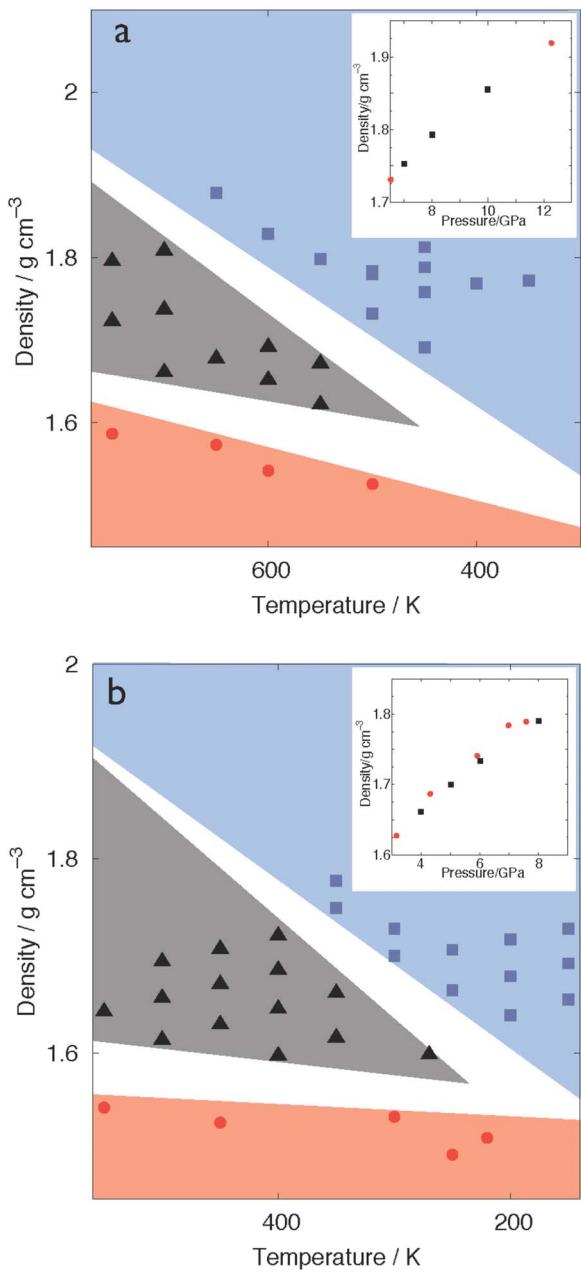
FIG. 3. (Color online) Density (g cm^{-3}) of (a) TIP5P and (b) TIP4P ice VII against $T(K)$ in descending order to compare with hard spherocylinder: Crystal, plastic, and liquid phases are represented by blue square, black triangle, and red circle, respectively. Insets, density against p(GPa) at (a) 500 K and (b) 300 K: Red circle, experiment; black square, corresponding MD simulation.

present simulations, which gives credibility of the classical potential functions.[22] Figure 3(a) shows the densities of three phases against temperature. The densities of ice VII at 500 K are compared to experiments and agreement is fairly good.[23] The region that the plastic phase is stable becomes smaller as the pressure is lowered. There are some gaps in the density plot that separate the plastic phase from the other two. This plot provides a rough overview on the stable region of the plastic state, although it should be taken into account that the boundaries obtained here are the upper limits of the lower temperature phases, where transitions are observed upon increasing temperature.

Although the TIP5P model is known to reproduce many properties of liquid water and ice, there is a possibility that the plastic phase is merely associated with this particular model of water. Thus, the second series of MD simulations are carried out for the TIP4P model,[10] which is composed of three charged sites and one LJ interaction site and is known to reproduce the phase diagram of water in a pressure range of 0–10 GPa.[11] Again, the transition to the plastic phase is observed. As shown in Fig. 3(b), the domain of the plastic for the TIP4P model is shifted to lower temperature region with respect to that for the TIP5P model. However, the basic features of the crystal-plastic and plastic-liquid transitions remain the same as those found for the TIP5P water. We also confirm that another frequently used potential for water, SPC/E,[16] results in the same conclusion (ice VII at 8 GPa transforms to plastic above 410 K). In short, the spontaneous formation of the plastic phase is observed for three potential models with fairly different parameters and, thus, the appearance of the plastic phase seems to be not a consequence of a specific model but rather an inherent character of water.

Thus far, we examined the upper limits of transformation temperature of ice VII and that of the plastic phase. Now, in the third series of MD simulations, we investigate thermodynamic properties and the phase behaviors in more detail. Three sets of MD simulations over wide ranges of temperature are carried out with initial structures of crystal, plastic, or liquid state at pressures of 6, 7, 8, and 10 GPa. Our focus is placed mainly on the properties at 10 GPa. A sequence of the phase transformations from ice VII to plastic phase and, finally, to liquid or the other way around is clearly seen in the densities, enthalpies, and potential energies plotted against temperature [Figs. 4(a)–4(c)]. Either quantity changes almost linearly with temperature in the ranges where three phases are stable. The crystalline phase, ice VII, transforms itself into the plastic state around 600 K, as observed in the first series of MD simulations. This change occurs suddenly and is accompanied by the significant amount of heat release and volume expansion. The jump in the enthalpy between 580 and 600 K (latent heat) is as large as that in the transition from ice Ih to liquid water at atmospheric pressure. The initial plastic phase is reverted back, within a few nanoseconds, to a crystalline structure when cooled down to temperatures below 590 K. The significant enthalpy and volume changes could be suggestive of the first order phase transition. Upon heating, the plastic is transformed to liquid with the enthalpy increase and the volume dilation at 890 K. The difference in potential energy between the plastic and liquid phase is much smaller than that in enthalpy, as shown in Fig. 4(c), indicating that the lower enthalpy in plastic arises from the smaller volume, not the lower energy, with respect to liquid. The liquid structure upon cooling remains metastable in a deeply supercooled region but finally freezes into the plastic state at 680 K. The large hysteresis means the first order phase transition between the liquid and the plastic state. Curves of the chemical potentials of plastic and crystalline phases intersect around 590 K and those of plastic and liquid intersect at 780 K, as shown in the inset of Fig. 4(d). Even at lower pressures, similar behaviors are observed but the domain of
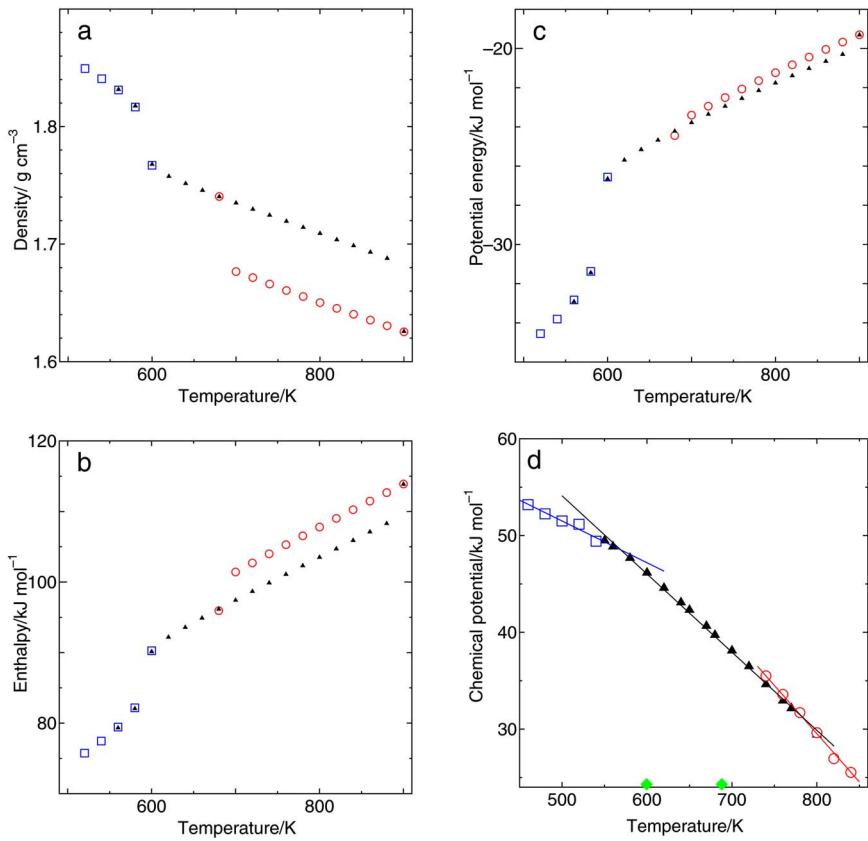
FIG. 4. (Color online) Thermodynamic properties of TIP5P water at 10 GPa: (a) Density in $g\,cm^{-3}$, (b) enthalpy, and (c) potential energy in $kJ\,mol^{-1}$ of water at 10 GPa whose initial structures are crystal (blue square), plastic (black triangle), and liquid (red circle) states. (d) Calculated chemical potentials of three phases together with the two experimental melting points (green diamond on the abscissa).

the plastic phase becomes smaller, as tabulated in Table I. (The error in density, enthalpy, and potential energy is less than the size of the symbols in Fig. 4.)

The heat ($\Delta H = 6.8\ kJ\,mol^{-1}$) from crystal to plastic at 10 GPa is much larger than that from plastic to liquid ($\Delta H = 3.9\ kJ\,mol^{-1}$), which is generally observed in plastic-forming substances.[12] Those values decrease with decreasing pressure. However, the entropy changes (12 and $5\ J\,mol^{-1}\,K^{-1}$, respectively) remain almost constant. On the other hand, the volume changes in both transformations are similar to each other. Thus, the crystal-plastic phase boundary, if any, in the T-p plane has a steeper slope than the plastic-liquid, and the plastic domain expands in the high-temperature and high-pressure region.

The structure factor is an appropriate quantity to discern existence of the long range order. Those for oxygen atoms and for hydrogen atoms in the three phases at 10 GPa are plotted in Figs. 5(a) and 5(b). The periodic structure on oxygen packing remains even in the plastic phase, but hydrogens have no definite arrangement except for the hydrogen-bond distance. The liquid has no sharp peak, indicating different phases from the others. The differences among three typical phases are much larger than those arising from the wide temperature difference in the same phase.

TABLE I. Temperatures of transitions between crystal and plastic (c-p) and between plastic and liquid (p-l) estimated by the chemical potential calculations.

Pressure (GPa)		7	8	10
Temperature (K)	(c-p)	500	555	595
	(p-l)	610	700	780

In a crystalline structure, each OH chemical bond orients roughly to one of $(\pm 1, \pm 1, \pm 1)$ directions, and a rotation from one of those orientations to another is suppressed by a free energy barrier much higher than $k_B T$, where $k_B T$ is the measure of the thermal energy. Once ice VII is transformed to the plastic phase, the barrier must be as low as $k_B T$. The normalized probability densities, $\rho(\theta, \phi)$, that an OH bond vector orients itself in between θ and $\theta + d\theta$ and between ϕ and $\phi + d\phi$ are obtained from the MD simulations. The free energy is calculated as $-k_B T \ln \rho$ and its minimum value is subtracted so as to compare the barrier height. The free energy barriers at 10 GPa along the path from the azimuthal angle $\phi = -\pi/4$ to $+\pi/4$ of OH bond in a molecule with the fixed polar angle $(\theta = \pi/4)$ are plotted in Fig. 6. The high free energy barriers of several $k_B T$ at 580 K become drastically lowered to levels less than $k_B T$ at 620 K.

A plastic phase appears in hard spherocylinder when the anisotropy is smaller than a certain magnitude, i.e., when it is close to sphere.[24] The anisotropy (an aspect ratio) in hard spherocylinder is intuitively related to the temperature in water because the anisotropic nature of water stemming from hydrogen bonds is more pronounced at lower temperature and, thus, inversely, high temperature corresponds to a small aspect ratio. In a phase diagram of the density-anisotropy for hard spherocylinders, a plastic phase region becomes larger with decreasing density but disappears completely at low density. This feature for the hard spherocylinder is similar to that for water in the density-temperature plane in Fig. 3(a) [and fig. 3(b)].

It is interesting to address why a molecule is allowed to make the facile rotation in the plastic phase. The potential
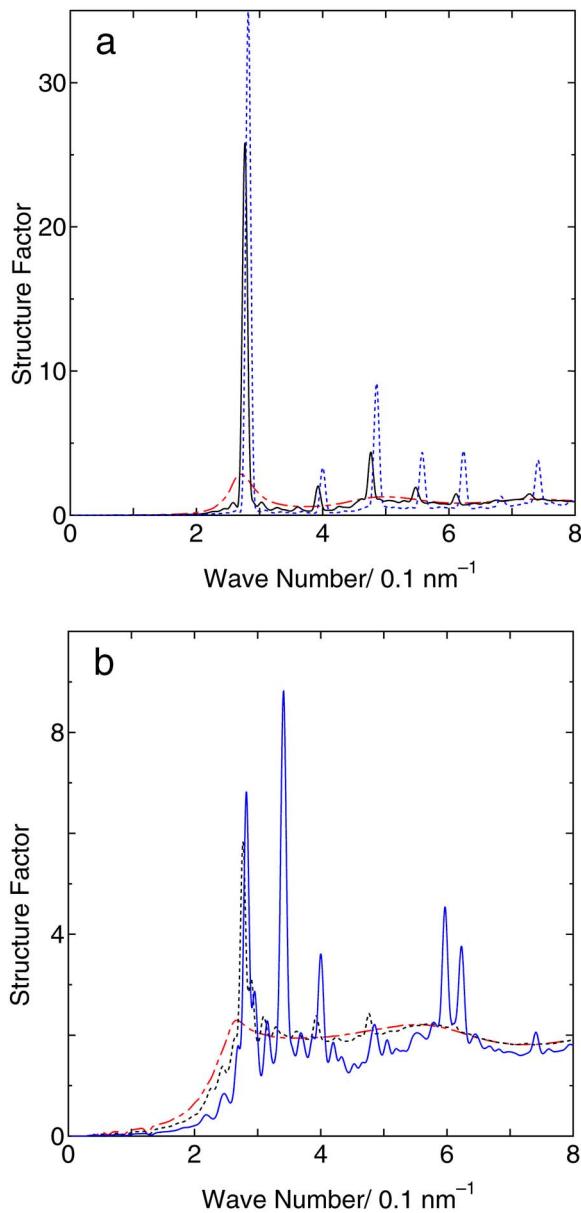
FIG. 5. (Color online) (a) Structure factor of OO distribution and (b) that of HH distribution for crystal at 550 K (blue, solid), plastic at 700 K (black, dotted), and liquid at 900 K (red, dash dot) for TIP5P model.

energy of an individual water molecule in the phase fluctuates, as plotted in Fig. 7, whose magnitude is as large as that in liquid state. These fluctuations have been known for liquid water at ambient condition and found to be mostly associated with the rotation caused by a kind of local frustration.[25] The hydrogen bonding percentage in the *inherent structure*[21] of plastic phase is approximately 66% with a hydrogen bond defined by an energetic criterion of $-16 \, \text{kJ} \, \text{mol}^{-1}$ as the threshold energy. This indicates that there are many frustrations (it is 100% in crystal and 62% in liquid). That is, connectivity of the hydrogen-bond network of the plastic phase is close to that in liquid. Thus, it is plausible that the mechanism of rotational motion in plastic phase is the same as that found in liquid water[25] where highly cooperative motions allow a large potential energy fluctuation of an individual molecule.
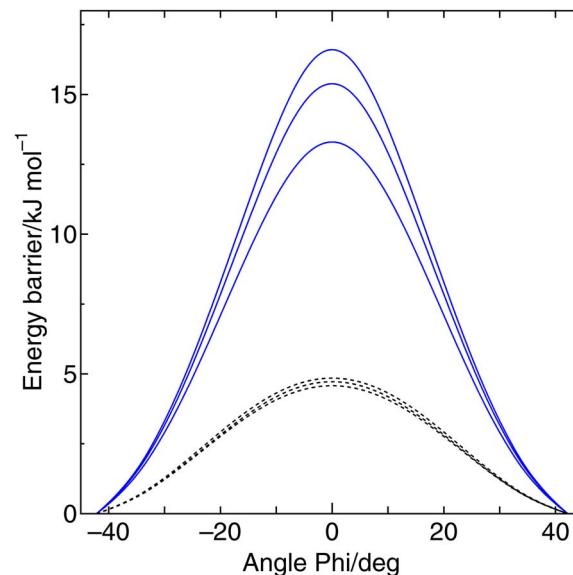
FIG. 6. (Color online) Free energy of TIP5P water molecule against azimuthal angle (ϕ) of an OH bond with a fixed polar angle (θ) of $\pi/4$ ($T=540-580$ K for crystal and $T=620-660$ K for plastic) at 10 GPa.

Individual water molecules in solid and plastic phases are bound to the lattice sites (with infrequent jumps to the other sites) executing vibrational motions. The mean amplitude increases with increasing temperature. The relative mean amplitude has been related to the onset of melting known as Lindemann's criterion.[26,27] It is 0.18 in bcc lattice as ice VII and 0.15 for face-centered cubic (fcc) lattice. In crystalline ice VII of TIP4P water, the relative mean amplitude of the vibrational motion is too small to melt it, as plotted in Fig. 8. It cannot reach Lindemann's criterion without passing through a plastic phase. However, there exists a large gap between crystalline and plastic states. No such a gap is observed in the other ice polymorphs, Ic or VI, and the amplitude increases smoothly to the melting temperature.
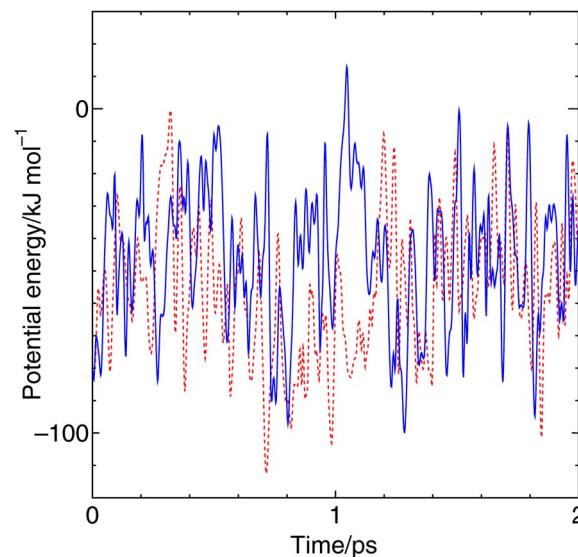
FIG. 7. (Color online) Time evolution of potential energy for individual water molecules over 2 ps in plastic (blue, solid) and liquid (red, dotted) states at 620 K and 10 GPa.
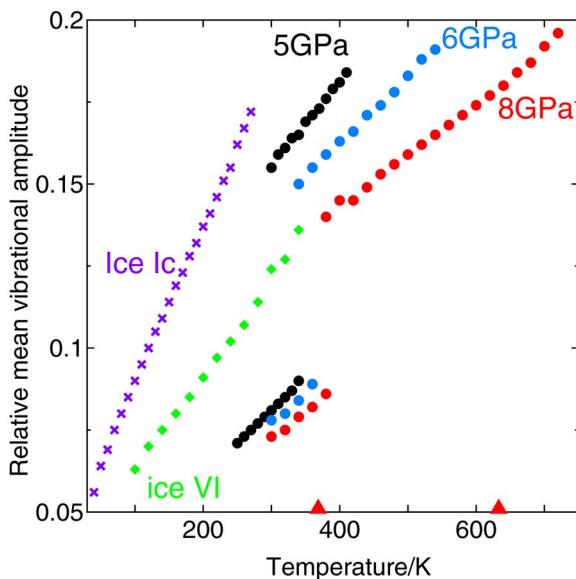
FIG. 8. (Color online) Relative mean amplitude of lattice vibrational motions of ice VII (including plastic phase) of TIP4P model at 5 GPa (blue triangle), 6 GPa (black circle), and 8 GPa (red square) together with those of ice Ic at 0.1 MPa (purple cross) and of ice VI at 2 GPa (green diamond) together with the two experimental melting points at 8 GPa (red triangle on the abscissa).

It is worthwhile to show robustness of the plastic phase with respect to varying potential parameters of a waterlike molecule. In particular, we focus on an effect of strength of hydrogen bonds on the domain of plastic state.[28] It turns out that a single scaling parameter q of the charge magnitudes of the TIP5P model ($q=1$ corresponding to the original and $q=0$ to no partial charges) provides useful information on the phase behaviors of water. MD simulations are performed for the modified TIP5P model with various q values at 10 GPa increasing T started from an ice VII structure. The resultant phases at a given q are depicted in Fig. 9. Obviously, the stable phase for $q=0$ in the limit of $T \rightarrow 0$ is a fcc-like plastic because the waterlike molecule with $q=0$ is a free rotor fixed at fcc lattice due to the LJ interaction. For $q=0.85$ or smaller, bcc crystal is transformed to fcc plastic upon heating, whereas for q greater than 0.85, the high-temperature phase is bcc plastic (although a phase behavior for $q=0.9-0.95$ is a little complicated). It should be noted that the existence of a
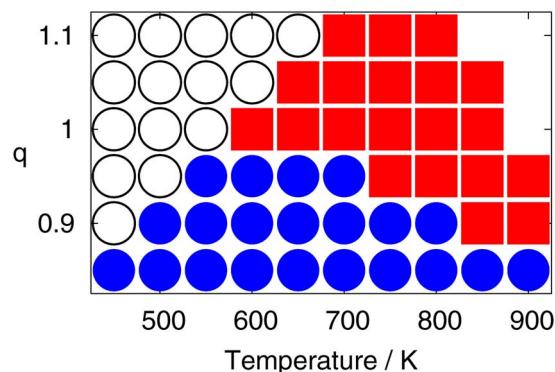
FIG. 9. (Color online) Phase behavior of TIP5P-like water in T-q (relative charge magnitude) space at 10 GPa. The phases are represented by symbols, open circle (bcc crystal), red square (bcc plastic), blue filled circle (fcc plastic), and blank (liquid).

plastic phase is confirmed for any q values examined. The charge magnitude for a real water is expected to fall into the q range examined here and, therefore, it is reasonable to speculate that real water has a plastic phase, too.

Hydrogen sulfide, which has a molecular geometry similar to water, is known to form a fcc plastic.[29] The hydrogen bond in H_2S is much weaker than that in water and so the packing effect outweighs the hydrogen bond in determining a lattice form. This is exactly what we find in the waterlike model with a reduced Coulombic interaction. The stronger Coulombic interaction gives rise to a bcc plastic in which hydrogen bonds play a significant role to maintain bcc structure.

The existence of the plastic phase may explain the discrepancy between experimental results on the ice VII–liquid phase boundary, which emerges around a few gigapascals and becomes larger with increasing pressure.[30,31] The large discrepancy in the melting curve of ice VII can be associated with a question why the plastic state has not been reported. In Fig. 4(d) (also in Fig. 8 at 8 GPa), the two different experimental melting points at 10 GPa are marked on the abscissa. Although the higher melting temperature experimentally measured is somewhat different from the melting temperature of the plastic phase in the simulation, it is evident that there is a large discrepancy in the experimental melting temperature. That two fairly different phase boundaries are observed in two different experimental studies is consistent with the existence of the plastic phase whose region increases with increasing temperature. Most of the recent experimental investigations on the melting was made by direct visualization,[31] while the earlier experiment detected the melting of ice VII by the volume change.[30] The different methods may detect the two different transitions, although other causes of the discrepancy such as technical difficulty at high pressure, hysteresis in cooling and heating processes, and purity of water are not ruled out.

Even if the number of water molecules is changed to 1024 and 3456, a plastic phase is recovered. Even when a simulation cell dimension is allowed to change in x, y, and z directions independently,[17,18] it remains cubic for three kinds of potentials in the course of simulation. It should be noted that the SPC/E water gives qualitatively the same results as the TIP5P. Only the TIP4P above 6 GPa gives rise to a rectangular cell in which molecular arrangement is fcc-like but it still possesses a plastic character. We also confirm that the two methods in the treatment of the long range interaction give rise to no appreciable difference in the results.

IV. CONCLUDING REMARKS

We present MD simulations on the plastic phase, in which individual water molecules make facile rotations as in liquid state but they are held tightly to the lattice sites. Molecular dynamics simulations of three models of water demonstrate that a plastic ice phase appears when ice VII is heated or liquid water is cooled at high pressures above several gigapascals. The plastic phase is stable within a timescale of simulations. It is found that a large amount of latent heat is absorbed when ice VII is transformed to the rotator

phase, which is a typical characteristic of the plastic transitions for nearly spherical molecules. In addition to the spontaneous formation of plastic phase in the simulations, its existence is supported by robustness of the plastic phase for hypothetical water with varying degrees of Coulombic interaction and appearance of a plastic phase in H_2S. The plastic phase is also consistent with the phase boundary of plastic phase for hard spherocylinders. Dissociation of water molecules takes place at high pressure, 30 GPa, and high temperature above 2000 K. Thus, it is reasonable to consider that   appearance of the plastic phase has nothing to do with the ionization of water.[22]

ACKNOWLEDGMENTS

[1] D. Eisenberg and W. Kauzmann, in *The Structure and Properties of Water* (Oxford University Press, Oxford, 1969).

[2] V. F. Petrenko and R. W. Whitworth, *Physics of Ice* (Oxford University Press, Oxford, 1999).

[3] O. Mishima and H. E. Stanley, Nature (London) **396**, 329 (1998).

[4] J. M. Besson, Ph. Pruzan, S. Klotz, G. Hamel, B. Silvi, R. J. Nelmes, J. S. Loveday, R. M. Wilson, and S. Hull, Phys. Rev. B **49**, 12540 (1994).

[5] M. Song, H. Yamawaki, H. Fujihisa, M. Sakashita, and K. Aoki, Phys. Rev. B **68**, 024108 (2003).

[6] K. Koga, G. T. Gao, H. Tanaka, and X. C. Zeng, Nature (London) **412**, 802 (2001).

[7] G. Hummer, J. C. Rasaiah, and J. P. Noworyta, Nature (London) **414**, 188 (2001).

[8] Y. Maniwa, H. Kataura, M. Abe, S. Suzuki, Y. Achiba, H. Kira, and K. Matsuda, J. Phys. Soc. Jpn. **71**, 2863 (2002).

[9] A. I. Kolesnikov, J.-M. Zanotti, C.-K. Loong, P. Thiyagarajan, A. P. Moravsky, R. O. Loutfy, and C. J. Burnham, Phys. Rev. Lett. **93**, 035503 (2004).

[10] W. L. Jorgensen, J. Chandrasekhar, J. D. Madura, R. W. Impey, and M. L. Klein, J. Chem. Phys. **79**, 926 (1983).

[11] E. Sanz, C. Vega, J. L. F. Abascal, and L. G. MacDowell, Phys. Rev. Lett. **92**, 255701 (2004).

[12] N. G. Parsonage and L. A. K. Sataveley, *Disorder in Crystals* (Clarendon, Oxford, 1978).

[13] S. Nosé, J. Chem. Phys. **81**, 511 (1984).

[14] H. C. Andersen, J. Chem. Phys. **72**, 2384 (1980).

[15] M. W. Mahoney and W. L. Jorgensen, J. Chem. Phys. **112**, 8910 (2000).

[16] H. J. C. Berendsen, J. R. Grigera, and T. P. Straatsma, J. Phys. Chem. **91**, 6269 (1987).

[17] D. Frenkel and B. Smit, *Understanding Molecular Simulation* (Academic, San Diego, 1996).

[18] D. C. Rapaport, *The Art of Molecular Dynamics Simulations* (Cambridge University Press, Cambridge, 1997).

[19] Y. Koyama, H. Tanaka, G. T. Gao, and X. C. Zeng, J. Chem. Phys. **121**, 7926 (2004).

[20] C. A. Angell, Annu. Rev. Phys. Chem. **43**, 693 (1992).

[21] F. H. Stillinger and T. A. Weber, Phys. Rev. A **25**, 978 (1982).

[22] E. Schwegler, G. Galli, F. Gygi, and R. Q. Hood, Phys. Rev. Lett. **87**, 265501 (2001).

[23] Y. Fei, H.-K. Mao, and R. J. Hemley, J. Chem. Phys. **99**, 5369 (1993).

[24] P. Bolhuis and D. Frenkel, J. Chem. Phys. **106**, 666 (1997).

[25] I. Ohmine and H. Tanaka, Chem. Rev. (Washington, D.C.) **93**, 2545 (1993).

[26] F. A. Lindemann, Z. Phys. **11**, 609 (1910).

[27] F. H. Stillinger, Science **267**, 1935 (1995).

[28] R. M. Lynden-Bell and P. G. Debenedetti, J. Phys. Chem. B **109**, 6527 (2005).

[29] M. J. Collins, C. I. Ratcliffe, and J. A. Ripmeester, J. Phys. Chem. **93**, 7495 (1989).

[30] O. Mishima and S. Endo, J. Chem. Phys. **68**, 4417 (1978).

[31] F. Datchi, F. P. Loubeyre, and R. LeToullec, Phys. Rev. B **61**, 6535 (2000).